Properties and structure-function relationships of veltuzumab (hA20), a humanized anti-CD20 monoclonal antibody

David M. Goldenberg,[1] Edmund A. Rossi,[2] Rhona Stein,[1] Thomas M. Cardillo,[2] Myron S. Czuczman,[3] Francisco J. Hernandez-Ilizaliturri,[3] Hans J. Hansen,[2] and Chien-Hsing Chang[2]

[1]Garden State Cancer Center, Center for Molecular Medicine and Immunology, Belleville, NJ; [2]Immunomedics, Morris Plains, NJ; and [3]Department of Medicine, Roswell Park Cancer Institute, Buffalo, NY

Veltuzumab is a humanized anti-CD20 monoclonal antibody with complementarity-determining regions (CDRs) identical to rituximab, except for one residue at the 101st position (Kabat numbering) in CDR3 of the variable heavy chain (V_H), having aspartic acid (Asp) instead of asparagine (Asn), with framework regions of epratuzumab, a humanized anti-CD22 antibody. When compared with rituximab, veltuzumab has significantly reduced off-rates in 3 human lymphoma cell lines tested, as well as increased complement-dependent cytotoxicity in 1 of 3 cell lines, but no other in vitro differences. Mutation studies confirmed that the differentiation of the off-rate between veltuzumab and rituximab is related to the single amino acid change in CDR3-V_H. Studies of intraperitoneal and subcutaneous doses in mouse models of human lymphoma and in normal cynomolgus monkeys disclosed that low doses of veltuzumab control tumor growth or deplete circulating or sessile B cells. Low- and high-dose veltuzumab were significantly more effective in vivo than rituximab in 3 lymphoma models. These findings are consistent with activity in patients with non-Hodgkin lymphoma given low intravenous or subcutaneous doses of veltuzumab. Thus, changing Asn_{101} to Asp_{101} in CDR3-V_H of rituximab is responsible for veltuzumab's lower off-rate and apparent improved potency in preclinical models that could translate into advantages in patients. (Blood. 2009;113:1062-1070)

Introduction

Advances in medical treatments during the past 10 years have witnessed the introduction of 9 antibodies for the therapy of diverse cancers.[1] Most of these new biologic therapeutics are combined with conventional cytotoxic drugs, indicating that the antibodies require additional measures to improve their efficacy.[1] This is best exemplified with rituximab, the first-generation chimeric anti-CD20 monoclonal antibody (mAb) that was approved initially as a monotherapy for the treatment of non-Hodgkin lymphoma (NHL).[2] On the basis of this success, efforts are under way to introduce improved anti-CD20 antibodies.[3-8]

Most of these new mAbs are intended to reduce the murine components while enhancing FcγR or complement-mediated functions.[8-10] One of the first second-generation mAbs developed to mitigate the infusion-related reactions experienced with rituximab is the hA20 mAb,[3] now termed veltuzumab, which has a shorter infusion time while indicating a higher complete response rate than has been reported for rituximab.[11,12] Veltuzumab was constructed recombinantly on the framework regions (FRs) of epratuzumab, the humanized anti-CD22 mAb or hLL2,[13] but has identical variable kappa light chain (V_k) complementarity-determining regions (CDRs), identical CDR1-variable heavy chain (V_H) and CDR2-V_H, except a different CDR3-V_H, compared with rituximab. Our initial characterization of veltuzumab[3] did not address whether these changes would result in different functions and therapeutic properties from those of rituximab. However, we postulated that, similar to the experience with epratuzumab,[14] it would be well tolerated during more rapid infusions than rituximab, which has been confirmed in monkeys, as shown herein, and in patients.[11,12] We now report that veltuzumab has unique characteristics in terms of significantly improved complement-dependent cytotoxicity (CDC) in 1 of 3 cell lines, slower off-rates in all 3 lymphoma cell lines tested, and significantly improved therapeutic results in vivo in 3 different lymphoma models, compared with rituximab, and potent anti–B-cell activity in cynomolgus monkeys, thus corroborating the activity observed in patients at very low doses. Surprisingly, we have determined that these differences between veltuzumab and rituximab, at least with regard to off-rates, are related to a single amino acid change in CDR3-V_H.

Methods

Antibodies

The development of veltuzumab has been described previously,[3] using the same human immunoglobulin G (IgG) donor FRs of epratuzumab.[13] Specifically, FR1, FR2, and FR3 of EU and FR4 of NEWM were selected for grafting the CDRs of V_H, and the FRs of REI were selected for grafting the CDRs of V_k. Key murine residues were retained in the FRs to maintain the binding specificity and affinity of veltuzumab for CD20 similar to those of the parental murine antibody (A20). The amino acid sequences of V_H and V_k are shown for A20, C2B8, and veltuzumab in Figure S1A,B (available

Submitted July 10, 2008; accepted September 28, 2008. Prepublished online as *Blood* First Edition paper, October 21, 2008; DOI 10.1182/blood-2008-07-168146.

The online version of this article contains a data supplement.

Presented in part at the 44th Annual Meeting of the American Society of Clinical Oncology, Chicago, IL, May 30-June 3, 2008.

The publication costs of this article were defrayed in part by page charge payment. Therefore, and solely to indicate this fact, this article is hereby marked "advertisement" in accordance with 18 USC section 1734.

Table 1. Comparison of CDR3-V_H

Kabat numbering	95					100						101	102
Veltuzumab	S	T	Y	Y	G	G	—	D	W	Y	F	D	V
D101N	●	●	●	●	●	●	—	●	●	●	●	N	●
CA20	●	●	●	●	●	●	—	●	●	●	●	●	●
Rituximab	●	●	●	●	●	●	—	●	●	●	●	N	●
1F5	●	H	●	G	S	N	Y	V	D	●	●	●	●

Residue marked as ● is identical to that of veltuzumab in the same position. Single letters represent amino acids.
— indicates not applicable.

on the *Blood* website; see the Supplemental Materials link at the top of the online article).

The chimeric form of veltuzumab, cA20, was generated by grafting the V_H and V_k domains of A20 to the human constant regions; thus, cA20 differs from veltuzumab in the variable FRs but has identical CDRs to veltuzumab. A mutant of veltuzumab, designated D101N, was engineered with a single amino acid change of aspartic acid (Asp_{101}) to asparagine (Asn_{101}) in CDR3-V_H; thus, D101N has the same CDRs as rituximab but identical FRs to veltuzumab. The construction of the expression vector for D101N is provided in Document S1.

Veltuzumab, cA20, D101N, 1F5, labetuzumab (hMN-14, humanized anti-CEACAM5 mAb), and WR2, a rat anti–veltuzumab-idiotype mAb, were provided by Immunomedics (Morris Plains, NJ). Rituximab and tositumomab (murine anti-B1) mAbs were obtained from commercial suppliers. Table 1 compares the CDR3-V_H of veltuzumab, cA20, D101N, rituximab, and 1F5, all of which have identical CDR1-V_H and CDR2-V_H sequences.

Cell lines

The murine hybridoma 1F5 and the human Burkitt lymphoma lines, Daudi, Raji, and Ramos, were purchased from ATCC (Manassas, VA). The non–Burkitt lymphoma cell lines were SU-DHL-6 from Dr Alan Epstein (University of Southern California, Los Angeles, CA), and WSU-FSCCL from Dr Mitchell Smith (Fox Chase Cancer Center, Philadelphia, PA). The cells were grown as suspension cultures in Dulbecco modified Eagle medium (DMEM; Life Technologies, Gaithersburg, MD), supplemented with 10% fetal bovine serum (FBS), penicillin (100 units/mL), streptomycin (100 μg/mL), and L-glutamine (2 mM).

Scatchard analyses

The maximum number of binding sites per cell and the apparent dissociation constants were determined by nonlinear regression analysis of the saturation binding data obtained with the radioiodinated samples and Raji cells, using Prism software (GraphPad Software, San Diego, CA).

In vitro cytotoxicity

The colorimetric [3-(4,5-dimethylthiazol-2-yl)-2,5-diphenyltetrazolium bromide] (MTT) assay, first described by Mosmann,[15] was used to evaluate the in vitro cytotoxicity by quantifying viable cells after treatments with anti-CD20 mAbs (5 μg/mL final concentration) for 4 days at 37°C in the absence or presence of goat anti–human (GAH) IgG (20 μg/mL final concentration).

Ex vivo depletion of B and T cells compared also with Daudi and Raji lymphoma cells

The effects of veltuzumab and rituximab on peripheral blood lymphocytes from healthy volunteers were evaluated ex vivo using flow cytometry. Blood specimens were collected under a protocol approved by the New England Institutional Review Board (Wellesley, MA) and informed consent was obtained in accordance with the Declaration of Helsinki. Heparinized whole blood (150 μL) was incubated with veltuzumab or rituximab for 2 days at 37°C and 5% CO_2 in a final volume of 250 μL. In some experiments, 5×10^4 Daudi or Raji cells were included in the mixture. Fluorescein isothiocyanate (FITC)–labeled anti-CD3, anti-CD19, anti-V_k, or mouse IgG_1 (isotype control), all purchased from BD Biosciences (San Jose, CA), were added to appropriate tubes, and incubation continued for an additional 30 minutes. Following lysing of erythrocytes, cells were analyzed using a FACSCalibur (BD Biosciences) with CellQuest software. Both Daudi and Raji cells separate from lymphocytes on forward scatter versus side scatter flow cytometry dot plots and are gated with the monocyte population. Daudi cells express high-surface V_k and are identified as κ-positive cells in the monocytes gate. Raji cells are identified as $CD19^+$ cells in the monocyte gate. The normal B cells are identified as $CD19^+$ cells in the lymphocyte gate. In these experiments, Student *t* test was used to evaluate statistical significance ($P \leq .05$).

Measuring antibody off-rates by flow cytometry

Veltuzumab, rituximab, cA20, D101N, 1F5, and tositumomab were labeled with phycoerythrin (PE) using an appropriate Zenon R-phycoerythrin IgG labeling kit (Z-25455; Molecular Probes, Invitrogen, Carlsbad, CA) following the manufacturer's protocol. Cells (Daudi, Raji, or Ramos) in 0.5 mL CM (phenol red–free RPMI 1640 media supplemented with 10% FBS) at 10^6 cells/mL were incubated with 5 μg of each PE-labeled mAb at room temperature for 30 minutes, pelleted at 400*g*, washed twice with CM, resuspended in 1.5 mL CM, and split into two 0.75-mL aliquots. To prevent rebinding, N-ethyl-maleimide (NEM)–blocked veltuzumab-Fab′ was added to each replicate (1 mg/mL final concentration), and the mean fluorescence intensity (MFI) was immediately measured to determine the maximal binding (T = 0) using a Guava PCA and Guava Express software (Guava Technologies, Hayward, CA). Subsequent measurements were taken at 30-minute intervals. The percentage maximal binding, which is the quotient of the MFI at T = X divided by that at T = 0, was plotted against time, and the results analyzed by Prism software to yield the half-life or off-rates.

CDC assays

Daudi, Raji, or Ramos cells (10^6/mL) were seeded (50 μL/well) in black 96-well plates (Nunc, Thermo Fisher Scientific, Rochester, NY) and incubated for 3 hours at 37°C and 5% CO_2 with each test mAb (0.001-10 μg/mL) in the presence of human complement (Quidel, San Diego, CA) at 1:20 final dilution. The indicator dye, AlamarBlue (BioSource, Camarillo, CA), was added and the incubation continued overnight. Viable cells were then quantified by measuring the fluorescence intensity with excitation at 530 nM and emission at 590 nM using a BioTek Synergy HT Multi-Detection Microplate Reader and KC4 Signature Software (BioTek Instruments, Winooski, VT). The dose-response curves generated from the mean of 6 replicate determinations were analyzed using Prism software to obtain half maximal effective concentration (EC_{50}) values. In the case of Daudi cells, to account for day-to-day variations in the assay, as well as to increase the precision of the EC_{50} estimates, the experiments used a multifactorial design, in which the assay for each antibody was performed in triplicate each day, and repeated on 3 different days for a total of 9 assays per antibody. The samples included 3 different lots of veltuzumab and 1 of rituximab. Statistical analysis of the EC_{50} data was based on a 2-way analysis of variance (ANOVA) model with day and antibody type as factors. A Dunnett multiple comparison procedure was used to perform the 3 comparisons of all 4 constructs at an overall experimental error rate of 0.05.

Antibody-dependent cellular cytotoxicity assays

Daudi cells were incubated with each test article in triplicate at 5 μg/mL for 30 minutes at 37°C and 5% CO_2. Freshly isolated peripheral blood

mononuclear cells (PBMCs) obtained from healthy volunteers were then added at a predetermined optimal effector-to-target ratio of 50:1. Following a 4-hour incubation, cell lysis was assessed by CytoTox-One (Promega, Madison, WI).

Tolerability and toxicokinetics in cynomolgus monkeys

An exploratory single- and repeated-dose study of intravenous and subcutaneous injections of veltuzumab was conducted in cynomolgus monkeys (*Macaca fascicularis*) at SNBL USA (Everett, WA). Sixteen male and 16 female monkeys weighing 2.5 to 6.6 kg (3-7 years old) were given intravenous or subcutaneous doses of 0, 6.7, 33.5, and 67 mg/kg (which correspond to 80, 375, and 800 mg/m^2 doses, respectively, in humans), either once or 3 times (2 weeks apart). The monkeys were examined regularly, with blood samples taken for mAb titers and pharmacokinetics (PK), blood chemistry, coagulation, and hematology testing, as well as urinalysis, and then postmortem evaluation of lymphoid tissue status in spleen, mandibular, and mesenteric lymph nodes.

Serum PK in mice after intraperitoneal or subcutaneous administration

Twelve 9-week-old naive female Swiss-Webster mice (Taconic Farms, Germantown, NY) were administered veltuzumab (150 μg in 200 μL) either intraperitoneally or subcutaneously. Serum samples were taken by retro-orbital bleeding at 0.5, 1, 4, 6, 24, 48, 120, 168, and 336 hours and stored frozen until analysis for veltuzumab, which involved capturing it with WR2-coated microtiter plates and quantifying the bound veltuzumab with a peroxidase-conjugated GAH polyclonal antibody (Jackson ImmunoResearch Laboratories, West Grove, PA). Noncompartmental analysis was performed on both the intraperitoneal and subcutaneous data, representing the best-fit model.

Evaluation of in vivo efficacy in mouse models

CB17 homozygous severe combined immune deficient (SCID) mice of approximately 20 g (7 weeks old when received from Taconic, Germantown, NY) were used for studies with Daudi and WSU-FSCCL lymphomas. For the Daudi model, mice were inoculated intravenously on day 0 with 1.5×10^7 cells, weighed, and randomly assigned to treatment and control groups. On day 1 or 5, mice received a single dose of veltuzumab subcutaneously or intraperitoneally, and those in the control groups received either saline (200 μL) or labetuzumab (60 μg). In addition to this study, a minimal effective dose experiment was performed in the same model; groups of 14 mice received a single dose of veltuzumab (0.5, 0.25, 0.1, or 0.05 μg) intraperitoneally, with saline given to controls. In the WSU-FSCCL follicular lymphoma model, each mouse (15/group) was inoculated with 2.5×10^6 cells intravenously, and 5 days later received a single dose of veltuzumab (0.035, 0.35, 3.5, or 35 μg) intraperitoneally.

Comparative studies of veltuzumab and rituximab also were conducted in the Daudi and WSU-FSCCL lymphoma models. Likewise, experiments were conducted at Roswell Park Cancer Institute (RPCI) comparing veltuzumab to rituximab under identical conditions in RPCI-bred SCID mice grafted with 10^5 Raji lymphoma cells via tail vein injection and treated with either mAb (10 mg/kg or 200 μg, total N = 15/group) administered intravenously 5, 10, 15, and 20 days after grafting.

Animals were monitored daily and killed humanely when hind-limb paralysis developed, when they became moribund, or if they lost more than 20% of initial body weight. Statistical differences in survival between treatment groups were analyzed using Kaplan-Meier plots (log-rank analysis of P values, which were considered significant at $P < .05$) provided by Prism software.

Effects of depleting natural killer cells and neutrophils on therapy

Depletion of natural killer (NK) cells and neutrophils was conducted as described.[16] Briefly, each mouse received 100 μL of anti–mouse Gr-1 ascites intraperitoneally and 100 μg anti–mouse interleukin-2 (IL-2) receptor antibody (TMβ-1; BD PharMingen, San Jose, CA) 1 day before inoculating 10^6 Raji cells, followed by 2 more intraperitoneal injections of anti–mouse Gr-1 ascites on days 6 and 13. Depletion was confirmed by fluorescence-activated cell sorting (FACS) analysis of blood samples taken from one depleted and one nondepleted mouse on days 3 and 13. Veltuzumab (200 μg) or saline was administered intravenously on days 3, 5, 7, and 11.

All animal studies were approved by the respective Institutional Animal Care and Use Committees of the Center for Molecular Medicine and Immunology and Roswell Park Cancer Institute, and performed in accordance with the Association for Assessment and Accreditation of Laboratory Animals, US Department of Agriculture, and Department of Health and Human Services regulations.

Results

Cell binding analyses

The number of binding sites per Raji cell and the apparent dissociation constants of veltuzumab were determined by direct cell surface saturation binding and Scatchard analyses and compared with those of rituximab. The results (Figure S2) confirm that both parameters are similar for veltuzumab and rituximab (2.0×10^5-4.2×10^5 vs 1.8×10^5-3.6×10^5 sites/cell, $P = .856$; 6.23-12.02 vs 6.70-8.63 nM; $P = .684$). These values are comparable to those reported previously by us[3] and others,[17] as well as in the prescribing information for rituximab.[18]

Off-rates

The dissociation of veltuzumab, rituximab, and cA20 from Daudi (Figure 1A), Ramos (Figure 1B), and Raji (Figure 1C) were compared in the presence of excess veltuzumab-Fab′-NEM at 37°C. Additional measurements were performed to compare the dissociation of veltuzumab, rituximab, and D101N from Raji (Figure 1D) under similar conditions. For each cell line tested, the half-life of veltuzumab on average was 2.7-fold (± 0.3) longer than that of rituximab ($P < .001$), but indistinguishable from that of cA20 ($P > .2$). In contrast, the D101N mutant dissociated from Raji cells with an off-rate 2- and 6-fold faster than rituximab and veltuzumab, respectively. These results suggest that the change of Asn_{101} to Asp_{101} is responsible for the slower dissociation of veltuzumab. We also compared the dissociation of veltuzumab, rituximab, D101N, 1F5, and tositumomab from Raji cells (Figure 1E) in the absence of the competing veltuzumab-Fab′-NEM, and found that veltuzumab has the longest half-life (281 minutes), followed by 1F5 (195 minutes), rituximab (94 minutes), tositumomab (50 minutes), and D101N (42 minutes).

In vitro antiproliferative activity

The ability of veltuzumab and rituximab to inhibit proliferation was examined on 4 lymphoma cell lines, SU-DHL-6, Daudi, Raji, and WSU-FSCCL, which differ in their expression levels of CD20,[3] using the MTT cell viability assay. While the sensitivity to both mAbs correlated with CD20 expression (SU-DHL-6 > Raji > Daudi > WSU-FSCCL), no significant differences in potency were observed between veltuzumab and rituximab within a cell line (Figure S3). Although cross-linking with GAH increased the efficacy of veltuzumab and rituximab on Raji and Daudi cells (both with intermediate levels of CD20 expression and sensitivity to killing by anti-CD20 mAbs), the addition of GAH did not further enhance the inhibition of proliferation of the highly sensitive SU-DHL-6 or the less sensitive WSU-FSCCL under the conditions tested.

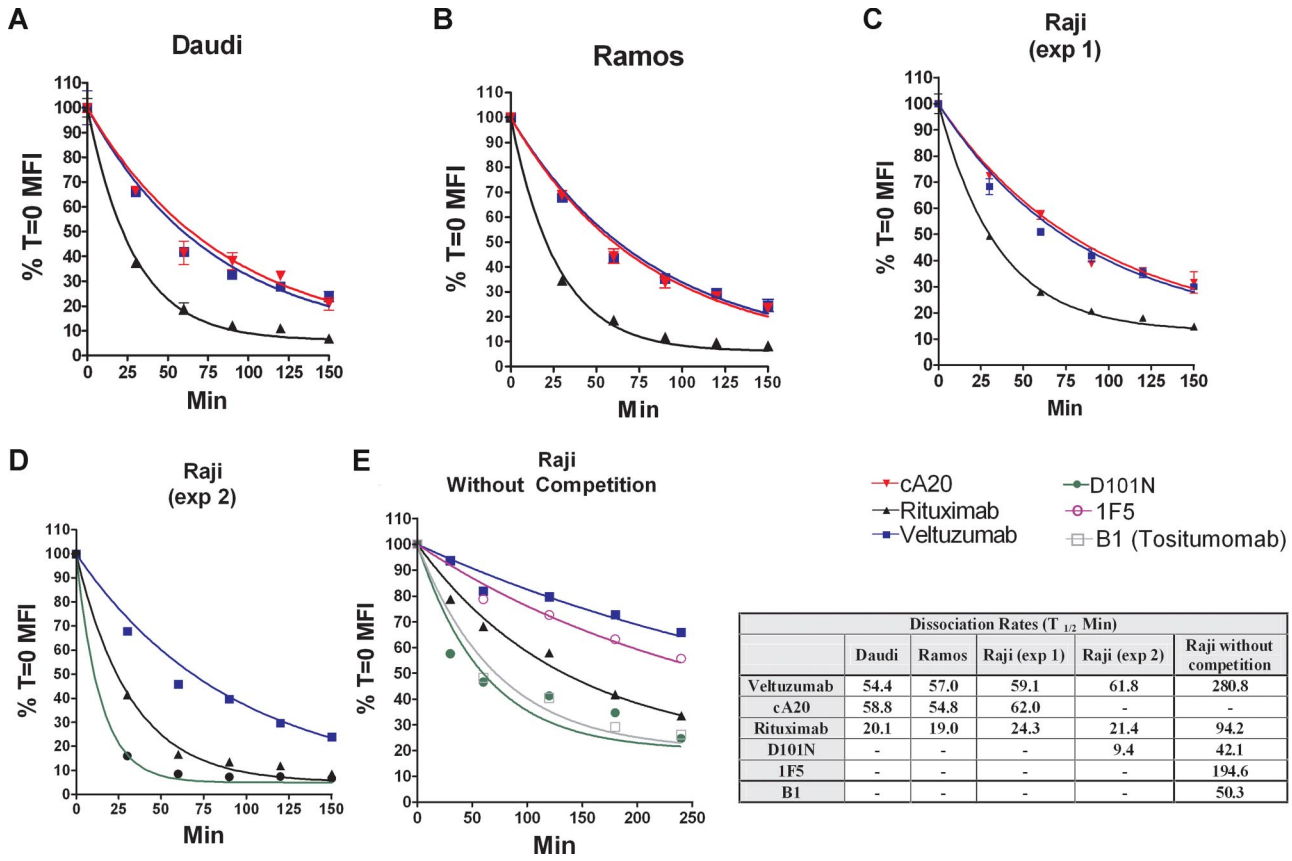

Dissociation Rates ($T_{1/2}$ Min)					
	Daudi	Ramos	Raji (exp 1)	Raji (exp 2)	Raji without competition
Veltuzumab	54.4	57.0	59.1	61.8	280.8
cA20	58.8	54.8	62.0	-	-
Rituximab	20.1	19.0	24.3	21.4	94.2
D101N	-	-	-	9.4	42.1
1F5	-	-	-	-	194.6
B1	-	-	-	-	50.3

Figure 1. Comparison of off-rates from live cells. Daudi (A), Ramos (B), and Raji (C-E) cells were stained with PE-labeled rituximab (△), veltuzumab (blue filled square), cA20 (red triangle), D101N (green filled circle), 1F5 (purple open circle) or B1 (gray open square). The labeled mAbs were incubated at 37°C with (A-D) or without (E) excess veltuzumab Fab′-NEM, and the cells were analyzed by flow cytometry over time. The off-rate was determined by nonlinear regression (one-phase exponential decay) and *P* values were generated by F test using GraphPad Prism software.

B- and T-cell and lymphoma depletion studies ex vivo

The effects of veltuzumab and rituximab on human peripheral blood lymphocytes of healthy volunteers were assessed ex vivo using flow cytometry. Aliquots of whole blood were incubated with the mAbs for 2 days, followed by FACS analysis of B cells ($CD19^+$) and T cells ($CD3^+$). Controls included no antibody and an isotype-matched, irrelevant antibody (labetuzumab). Incubation of whole blood with veltuzumab at 5 and 1 μg/mL led to a statistically significant ($P < .05$) decrease of 26% to 80% and 11% to 61%, respectively, in the number of B cells (Figure 2A), but not T cells (data not shown). Similar results were obtained using rituximab (data not shown). Because whole blood was used in the incubation mixtures, the decreases observed in the cell counts could be due to CDC, antibody-dependent cellular cytotoxicity (ADCC), as well as direct apoptotic signaling.

Figure 2B compares the depletion of human B cells versus Raji lymphoma cells by veltuzumab and rituximab, showing that both mAbs have virtually identical effects, including depleting normal B cells proportionately less than Raji lymphoma cells. Similar results were obtained in a comparison with Daudi lymphoma cells (data not shown).

CDC

With Daudi as the target cells for CDC, we observed consistently a lower value of EC_{50} for veltuzumab (Table 2) when compared with rituximab. Further measurements addressing any effect of day-to-day variation as well as any differences in EC_{50} patterns among the antibodies across different days indicated that the mean difference in EC_{50} observed between rituximab and each of the 3 lots of veltuzumab was consistently statistically significant ($P < .001$).

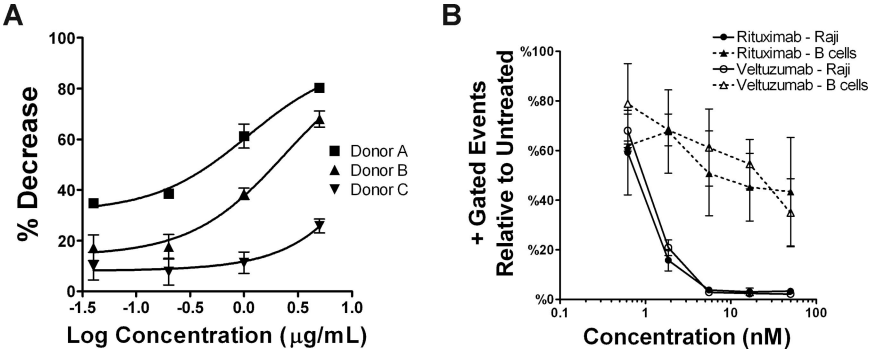

Figure 2. Ex vivo depletion of B cells and lymphoma cells. (A) The effect of veltuzumab on peripheral blood lymphocytes from healthy volunteers was evaluated in vitro using flow cytometry. Decrease in the percentage of $CD19^+$ cells present in the lymphocyte gate after a 2-day incubation of heparinized whole blood of healthy volunteers with veltuzumab is shown. Each line represents a different blood donor. Error bars, standard deviation. (B) The effects of veltuzumab and rituximab on peripheral blood B cells and Raji lymphoma cells are shown as the number of $CD19^+$ events relative to untreated cell mixtures. B cells are derived as the $CD19^+$ cells in the lymphocyte gate, while Raji cells are located in the monocytes gate. Error bars indicate standard deviation.

Table 2. Comparison of veltuzumab versus rituximab: summary of CDC results (EC_{50}) in the Daudi cell line

Antibody	No. of experiments	EC_{50}, μg/mL, mean ± SD	Mean difference, Vmab − Rmab	95% CI*
Rituximab	9	0.1485 ± 0.0200		
Veltuzumab, lot 1	9	0.0990 ± 0.0232	−0.0495	(−0.0611, −0.0378)
Veltuzumab, lot 2	9	0.0843 ± 0.0215	−0.0642	(−0.0758, −0.0525)
Veltuzumab, lot 3	9	0.0904 ± 0.0239	−0.0581	(−0.0697, −0.0464)

*Based on 2-way ANOVA model adjusted for multiple comparisons using the Dunnett method.

However, no differences between veltuzumab and rituximab were observed with CDC results in the other 2 cell lines, Raji and Ramos.

ADCC

With PBMCs as effector cells for ADCC, veltuzumab and rituximab produced similar extents of cell lysis (40%-45%; $P = .12$), which were significantly higher ($P < .001$) than labetuzumab (9.9%; data not shown).

PK studies in mice

While serum concentrations and clearance of veltuzumab were very similar between those animals injected intraperitoneally and subcutaneously (Figure S4), several of their respective PK-parameters were significantly different (Tables S1,S2). In terms of maximum serum concentrations (C_{max}) and the time to C_{max} (T_{max}), there were no significant differences between the injection routes. This was also true for comparisons between clearance (Cl) and area under the curve (AUC) values. However, notable differences were observed in the terminal half-life ($t_{½}$) and mean residence time (MRT), with the intraperitoneal route yielding significantly higher values for each ($P = .032$ and $P = .036$, respectively).

PK results of veltuzumab in normal mice are summarized in Document S1. After injecting 150 μg veltuzumab into these 30-g mice, we achieved a C_{max} of 30 μg/mL, or 5.3-fold less than what could be expected maximally. These findings suggested that we could inject 50 ng (0.05 μg or 0.0025 mg/kg) into an approximately 20-g tumor-bearing SCID mouse for our lowest therapy dose, which under ideal conditions would provide a maximum serum concentration of 87.7 ng/mL, that could yield an estimated C_{max} concentration of approximately 16.5 ng/mL veltuzumab in the serum (87.7 ng/mL divided by 5.3).

Tolerabilility and PK studies in cynomolgus monkeys

Veltuzumab administered intravenously or subcutaneously as single or multiple doses was well tolerated, with no clinical or persistent laboratory test abnormalities noted other than B-cell depletion in the circulation and lymphatic organs. Postmortem changes in the animals receiving all doses included follicular lymphoid depletion of the spleen, mandibular lymph nodes, and mesenteric lymph nodes at all doses (data not shown). Transient decreases in white blood cells, neutrophils, lymphocytes, and basophils were noted, but only a rapid reduction in the number of peripheral blood B cells was observed (results not shown). These effects occurred within 2 days of dosing by either route and were present at doses of 6.7 mg/kg or higher. The animals recovered either at 28 days when treated once or at 56 days when given 3 doses. PK analyses (data not shown) indicated that the half-life was estimated to be 5 to 8 days after intravenous injection or 6 to 13 days after subcutaneous administration, and the T_{max} for both routes ranged from 2 to 5 days. C_{max} following intravenous injection was linear and showed no accumulation, and the $AUC_{0\text{-}27\ days}$ was greater for intravenous administration than for the subcutaneous route. This is likely related to the longer period required for the mAb to enter the blood subcutaneously with a similar rate of clearance. The mean volume of distribution was greater after subcutaneous administration than after intravenous infusion at all dose levels (not shown). These results indicate that at the lowest single dose of 6.7 mg/kg (equivalent to 80 mg/m^2 in humans), rapid depletion of peripheral and splenic B cells occurs for veltuzumab given either by intravenous or subcutaneous routes at this low dose.

Burkitt lymphoma xenografts: intraperitoneal versus subcutaneous therapy

Mice bearing disseminated disease were treated with single intraperitoneal or subcutaneous injections of veltuzumab. All 3 doses (5, 20, and 60 μg, or 0.25, 1.0, and 3.0 mg/kg, respectively), regardless of the method administered, significantly increased survival of mice in comparison to the saline and labetuzumab control groups ($P < .001$). Comparisons between equal doses administered intraperitoneally and subcutaneously did not yield significant differences (Figure 3A). While the control mice succumbed to disease (hind-limb paralysis) on day 28, the mean survival times (MSTs) of the two 60-μg groups were 101.9 plus or minus 26.8 days and 114.6 plus or minus 21.8 days for intraperitoneal and subcutaneous, respectively, with 4 of 8 and 6 of 8 mice still alive when the study ended on day 126. Similar results were obtained for the animals given 20 μg, with the MSTs of 116.4 plus or minus 14.0 days (intraperitoneal) and 108.4 plus or minus 26.2 days (subcutaneous), and 5 of 8 mice alive at the end of the study in both groups. Only at the lowest dose (5 μg, or 0.25 mg/kg) was a greater than 50% mortality rate observed (3/8 and 1/8 mice were still alive at the end of the study in each intraperitoneal/subcutaneous group), but these mice still had a greater than 3.2-fold increase in the MSTs (91.1 ± 30.9 days and 91.6 ± 22.5 days for intraperitoneal and subcutaneous administration, respectively) compared with controls.

Minimum effective dose of veltuzumab in Daudi lymphoma xenografts

Since a single 5-μg dose of veltuzumab proved to be potent in the Daudi disseminated Burkitt lymphoma model, still lower doses (0.5, 0.25, 0.1, and 0.05 μg) were examined. Remarkably, all 4 doses improved survival significantly ($P < .001$) when compared with saline control mice (Figure 3B). For example, mice receiving a single dose of 0.5 μg (0.025 mg/kg) had a 3-fold improvement in the MST compared with controls (69.5 ± 23.9 days vs 21.4 ± 1.1 days). Even the lowest tested dose of 0.05 μg (50 ng, or 0.0025 mg/kg) increased the MST (50 ± 8 days) by more than 2-fold over the controls.

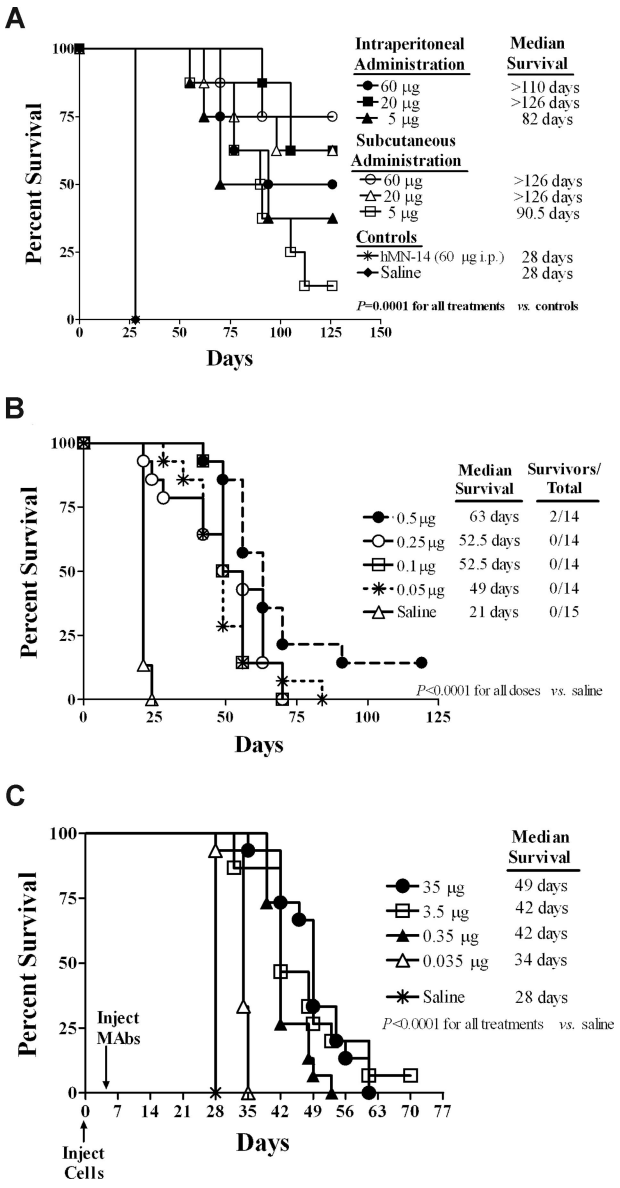

Figure 3. Evaluation of in vivo efficacy in mouse models. (A) Survival of mice in a disseminated Burkitt lymphoma xenograft model was compared for veltuzumab treatment via intraperitoneal versus subcutaneous administration. SCID mice were administered 1.5×10^7 Daudi cells intravenously on day 0. Therapy with veltuzumab began on day 1 with mice receiving either a single intraperitoneal or single subcutaneous injection of veltuzumab at does of 60, 20, or 5 μg. Control mice received an intraperitoneal injection of either saline or 60 μg hMN-14 IgG (labetuzumab, anti-CEACAM5 isotype-matched antibody). (B) The minimal effective dose of veltuzumab was determined in a disseminated Burkitt lymphoma xenograft model. SCID mice were administered 1.5×10^7 Daudi cells intravenously on day 0. Therapy with veltuzumab began on day 1 with a single intraperitoneal injection of veltuzumab. Doses administered were 0.5, 0.25, 0.1, or 0.05 μg veltuzumab. Control mice received a 200-μL intraperitoneal injection of saline. (C) Survival of mice bearing disseminated follicular cell lymphoma was examined for treatment with decreasing doses of veltuzumab. SCID mice were administered 2.5×10^6 WSU-FSCCL cells intravenously on day 0. On day 5, mice received a single intraperitoneal injection of veltuzumab at a dose of 35, 3.5, 0.35, or 0.035 μg. Control mice received only saline.

Minimum effective dose of veltuzumab in follicular cell lymphoma xenografts

In disseminated follicular cell lymphoma, WSU-FSCCL, xenografts, mice were administered a single dose of veltuzumab (35, 3.5, 0.35, and 0.035 μg) intraperitoneally, 5 days after tumor inoculation. All 4 doses improved survival of the mice significantly ($P < .001$) when compared with the saline controls (Figure 3C). The MST of mice administered the 35-μg dose (44.3 ± 4.9 days) was not significantly different from that of the 3.5-μg group (39.5 ± 4.6 days), but was significantly ($P < .021$) longer than that of the 0.35- and 0.035-μg (35 ng or 0.002 mg/kg) groups (40.5 ± 1.6 days and 33.3 ± 2.1 days, respectively).

Comparative therapeutic effects of veltuzumab and rituximab

Studies in Daudi, WSU-FSCCL, and Raji tumor models showed statistically significant improved survival of veltuzumab over rituximab. The MST of 0.05 and 0.1 μg single doses (0.0025 and 0.005 mg/kg, respectively) given 1 day after grafting were 28 and 35 days versus 24 and 28 days for veltuzumab and rituximab, respectively ($P = .001$) in the Daudi Burkitt lymphoma, and also at the single low dose of 0.035 μg (0.0021 mg/kg) given 5 days after transplantation of the WSU-FSCCL model ($P = .005$; data not shown). Figure 4A shows the results of treating SCID mice with Raji lymphoma cells after administering veltuzumab or rituximab, indicating a statistically significant survival advantage for veltuzumab ($P = .002$), where median survival of veltuzumab was not reached, but rituximab-treated animals showed a median survival of 48 days after receiving 3 doses of 10 mg/kg (200 μg) on days 5, 10, 15, and 20 after tumor transplantation.

Effect of depleting NK cells and neutrophils on anti-lymphoma activity

We also examined the role of effector cells on veltuzumab's inhibition of Raji tumor growth in vivo (Figure 4B). In those animals depleted of NK cells and neutrophils, there was no difference between saline control and treated mice, both having the same MST (16.4 ± 1.3 days). In the nondepleted group, veltuzumab-treated mice had a significantly improved MST over the saline controls (38.6 ± 7.3 days vs 18.4 ± 0.9 days; $P < .004$).

Discussion

Due to our observations that rituximab combined with epratuzumab showed increased complete responses in NHL patients, with no increased side-effects over those resulting from monotherapy with rituximab,[14,19-21] our original purpose was to develop a humanized anti-CD20 mAb that could be combined with epratuzumab, but would be more tolerable for rapid infusions due to having the FRs of epratuzumab. The first characterization of veltuzumab reported similarities to rituximab in terms of epitope binding, affinity, ADCC, CDC, and cell growth inhibition in vitro.[3] Treating patients with NHL demonstrated a favorable tolerability and infusion profile, but also a high rate of complete responses (CR/CRu). The phase I/II trial in 82 NHL patients is now being summarized for publication, but it has been reported already that the complete response rates for all doses tested (27% for all follicular lymphoma patients for doses between 80 and 750 mg/m^2 once weekly times 4 weeks)[11,12] exceed those reported for repeated use of rituximab at its conventional dose in comparable patients.[22] Ongoing studies also showed that single absolute doses of 80 mg of veltuzumab induced rapid B-cell depletion in patients with NHL or immune thrombocytopenic purpura, including reversal of thrombocytopenia in the latter patients (data on file, Immunomedics). These findings prompted us to re-evaluate the functional properties of veltuzumab, also in comparison to rituximab, which is the subject of this article.

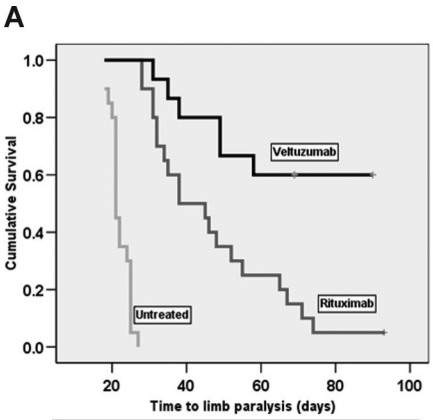

Treatment	Median (Days)			
	Estimate	Std. Error	95% Confidence Interval	
			Lower Bound	Upper Bound
Untreated	21	.318	20.37	21.62
Rituximab	38	7.454	23.391	52.60
Veltuzumab	Not Reach (NR)		NR	NR

Veltuzumab vs. Rituximab P = .002

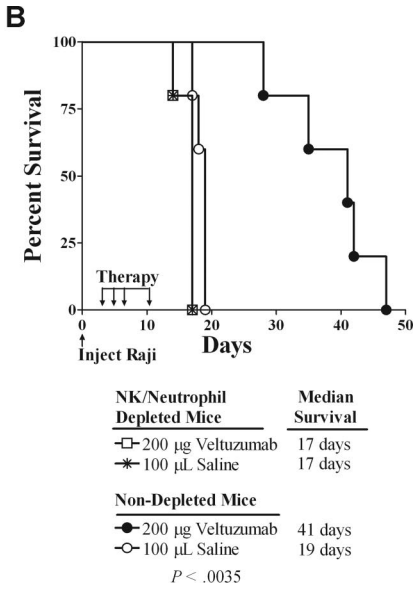

Figure 4. In vivo effects of veltuzumab compared with rituximab and after NK/neutrophil depletion in Raji lymphoma model. (A) Comparison of therapeutic effects on survival of RPCI-SCID mice bearing Raji lymphoma cells treated with 10 mg/kg veltuzumab or rituximab (or untreated control) on days 5, 10, 15, and 20 after tumor inoculation intravenously ($N = 15$ per group), indicating significantly improved survival ($P = .005$) of the veltuzumab group compared with the rituximab group. (B) The effect of depleting NK cells and neutrophils on anti-lymphoma activity in SCID mice. Veltuzumab therapy consisted of 200 μg given intravenously on days 3, 5, 7, and 11; control mice received 100 μL saline. Depletion of NK cells and neutrophils abrogated the anti-lymphoma activity of veltuzumab.

Studies in cynomolgus monkeys have now confirmed the effects of various intravenous and subcutaneous doses, showing that a single dose as low as the equivalent of 80 mg/m^2 in humans, given by either route, is sufficiently potent to induce peripheral blood and lymphatic organ B-cell depletion. In addition, enhanced survival and even cures were demonstrated in mice bearing CD20$^+$ lymphoma xenografts after a single ip or sc dose as low as 0.035 or 0.050 μg (or ~0.002 mg/kg). In these mouse studies, a dose-response was observed, but no significant difference between the intravenous or subcutaneous routes was noted.

In studies involving 3 lymphoma models in SCID mice, comparisons of low and high, single or multiple, doses showed a significantly increased survival time after veltuzumab compared with rituximab treatment, as conducted in 2 different laboratories. However, this was not consistent with ex vivo cell studies showing equal potency of veltuzumab and rituximab in killing human B cells and either Daudi or Raji lymphoma cells, but it is interesting that both antibodies were more effective against the tumor cells than the normal human B cells, suggesting that there may be a higher density of CD20 on these lymphoma cells.

Although different anti-CD20 mAbs have shown some variations in functional properties and epitope specificities, mediating different CDC and cell-killing effects,[23] virtually all recognize the large, extracellular loop and partially or completely crossblock each other,[24-26] except ofatumumab, which is reported to bind to a novel epitope of CD20.[27] Veltuzumab crossblocks binding by rituximab,[3] suggesting either the same epitope is recognized by both mAbs or binding to an adjacent epitope could result in steric hindrance.

In this study, the binding and dissociation parameters of veltuzumab and rituximab were compared both by Scatchard analyses and off-rate measurements. Scatchard analyses confirmed that veltuzumab and rituximab have similar affinity for cell-surface CD20 and number of binding sites per cell. Interestingly, statistical differences between veltuzumab or cA20 versus rituximab or D101N were found in a slower off-rate (ie, longer cell-surface retention) in all 3 human lymphoma cell lines tested, and a higher CDC-mediated cell killing in Daudi lymphoma cells (but not Raji and Ramos cells) by veltuzumab, compared with rituximab or D101N. Whether measured in the presence or absence of a competitive binder, veltuzumab and cA20, both containing Asp_{101} instead of Asn_{101} in CDR3-V_H, had significantly ($P < .001$) slower off-rates (~2.5-fold) than rituximab or D101N. The demonstration of CDC activity for veltuzumab in Daudi being significantly more than rituximab or D101N is also intriguing, since the Fc portion of veltuzumab is derived from that of epratuzumab, which fails to show CDC functions.[27] This suggests that rapid internalization of epratuzumab may prevent it from residing on the cell surface long enough to form membrane attack complexes needed for CDC. Our results also suggest that the off-rate difference between veltuzumab and rituximab is not related to the enhanced CDC observed in Daudi cells, as first postulated for ofatumumab,[4] since this difference was not observed for CDC in 2 other cell lines (Raji and Ramos) that also showed a significantly slower off-rate with veltuzumab compared with rituximab. Although these findings with veltuzumab involve evidently a different targeted epitope of CD20 than ofatumumab,[28] we are not convinced that such off-rate changes are due to the position of the epitope, as postulated by these authors. Nevertheless, we agree with Teeling et al[4] that such off-rate changes, as also described herein, may explain an antibody functioning at lower concentrations than other mAbs, such as we have found with veltuzumab, but whether CDC plays a role remains speculative.

It is doubtful that these differences are related to veltuzumab having the FRs of epratuzumab. The V_H and V_K chains of cA20 differ from those of rituximab in 6 positions, but except for the 101-residue in CDR3-V_H, the remaining 5 residues (2 in FR4-V_H and 3 in FR1-V_K) are unlikely to be responsible for the differential off-rates. Du et al reported a weaker interaction of the CDRs of another anti-CD20 mAb, c2H7, compared with rituximab, suggesting that the amino acid residues of 2H7 at the equivalent positions in CDR3-V_H have more bulky side chains, resulting in a wider pocket to accommodate the CD20 peptide.[29] The fact that cA20 and veltuzumab have virtually the same affinity and off-rate, whereas cA20 has more similar FRs to rituximab than to veltuzumab, emphasizes the more critical role of CDRs than FRs in interacting with CD20. Thus, the significant difference observed in the off-rate between veltuzumab/cA20 and rituximab/D101N is apparently due to the single amino acid difference in CDR3-V_H, and not to the

more extensive differences in the FRs between veltuzumab and rituximab. Accordingly, we believe this is the first single amino-acid change in a CDR that is shown to cause a functional effect, possibly resulting in a more potent antibody.

As discussed already, these in vitro off-rate and CDC differences are comparable to the findings with another anti-CD20 mAb, ofatumumab, which was reported to bind to a different epitope than rituximab,[28] and claimed to be therapeutically more active than rituximab in vitro.[4] However, this is not consistent with the relatively high doses chosen for clinical studies, also requiring long infusion times like rituximab,[30,31] or the lowest dose of 0.5 mg/kg (10 μg/mouse) shown to elicit growth inhibition in lymphoma xenografts.[31,32]

Still another recently developed human anti-CD20 mAb, GA101, which has properties of a type-II anti–CD20 mAb,[6] has been shown to be more potent in vitro and in animal models than rituximab, when mice were given repeated doses of 10 to 30 mg/kg.[6] This translates to each dose of repeated applications being between 200 and 600 μg in a 20-g mouse, which are at least 5000- to 15 000-fold higher than the single doses of 0.05 to 0.35 μg (0.002 mg/kg) of veltuzumab showing high antigrowth activity in the lymphoma xenografts tested. Depletion of murine NK cells and neutrophils prevented these effects of veltuzumab, emphasizing the role of ADCC in vivo, as shown previously for rituximab.[16]

In conclusion, in vitro, mouse, monkey, and other human studies indicate that (1) veltuzumab is active at a fraction of the conventional clinical dose of rituximab or of the minimal therapeutic doses of 2 other second-generation anti-CD20 mAbs in preclinical models; (2) survival studies in 3 different lymphoma models showed a significantly higher potency of veltuzumab over rituximab; (3) the 2 distinguishing differences in activity versus rituximab in vitro involve CDC and off-rate functions; and (4) the lower off-rate appears to be related to a single amino acid mutation at the Kabat-101 residue in the CDR3-V_H. This is the first description, to our knowledge, of a single amino acid difference in an antibody's CDR affecting its function, but whether this functional change in veltuzumab depends specifically on Asp_{101} or can be reproduced with other amino acid substitutions is of interest to investigate.

Acknowledgments

We thank Dr Nick Teoh for statistical advice on CDC studies; Dr Henry Founds for assistance in analyzing monkey data; and Diana Pilas, Roberto Arrojo, Anju Nair, Preeti Trisal, and Susan Chen for excellent technical support.

This work was supported in part by National Cancer Institute grant P01-CA103985 from the National Institutes of Health.

Authorship

Contribution: D.M.G., E.A.R., R.S., H.J.H., and C.-H.C. designed research, analyzed data, and wrote the paper; and T.M.C., M.S.C., and F.J.H.-I. performed research, collected and analyzed data, and revised the paper.

Conflict-of-interest disclosure: D.M.G., E.A.R., T.M.C., H.J.H., and C.-H.C. have employment, stock, and/or stock options with Immunomedics Inc, which owns and has patented veltuzumab. The remaining authors declare no competing financial interests.

Correspondence: David M. Goldenberg, Center for Molecular Medicine and Immunology, 520 Belleville Avenue, Belleville, NJ 07109; e-mail: dmg.gscancer@att.net.

References

1. Sharkey RM, Goldenberg DM. Targeted therapy of cancer: new prospects for antibodies and immunoconjugates. CA Cancer J Clin. 2006;56:226-243.
2. Castillo J, Winer E, Quesenberry P. Newer monoclonal antibodies for hematological malignancies. Exp Hematol. 2008;36:755-768.
3. Stein R, Qu Z, Chen S, et al. Characterization of a new humanized anti-CD20 monoclonal antibody. IMMU-106, and its use in combination with the humanized anti-CD22 antibody, epratuzumab, for the therapy of non-Hodgkin's lymphoma. Clin Cancer Res. 2004;10:2868-2878.
4. Teeling JL, French RR, Cragg MS, et al. Characterization of new human CD20 monoclonal antibodies with potent cytolytic activity against non-Hodgkin lymphoma. Blood. 2004;104:1793-1800.
5. Vugmeyster Y, Beyer J, Howell K, et al. Depletion of B cells by a humanized anti-CD20 antibody PRO70769 in *Macaca fascicularis*. J Immunother. 2005;28:212-219.
6. Umana P, Moessner E, Grau R, et al. GA101, a novel therapeutic type II CD20 antibody with outstanding anti-tumor efficacy in non-Hodgkin lymphoma xenograft models and superior B cell depletion. Ann Oncol. 2008;19(suppl 7):abstract 98.
7. Forero A, De Vos S, Pohlman B, et al. Preliminary results of a Phase I study of AME-133v, an Fc-engineered humanized monoclonal antibody, in low-affinity FcγRIIIa patients with previously-treated follicular lymphoma. Proc 99th Ann Meeting of the Am Assoc Cancer Res. 2008;abstract LB-70.
8. Glennie MJ, French RR, Cragg MS, Taylor RP. Mechanisms of killing by anti-CD20 monoclonal antibodies. Mol Immunol. 2007;44:3823-3837.
9. Maloney DG. Follicular NHL: from antibodies and vaccines to graft-versus-lymphoma effects. Hematology Am Soc Hematol Educ Program. 2007;226-232.
10. Martin P, Furman RR, Ruan J, et al. Novel and engineered anti-B-cell monoclonal antibodies for non-Hodgkin's lymphoma. Semin Hematol. 2008;45:126-132.
11. Morschhauser F, Leonard JP, Fayad L, et al. Low doses of humanized anti-CD20 antibody, IMMU-106 (hA20), in refractory or recurrent NHL: phase I/II results. Proc Am Soc Clin Oncol, J Clin Oncol. 2007;25:449s(abstract 8032).
12. Goldenberg DM, Chang C, Rossi EA, et al. Laboratory and clinical studies of high anti-lymphoma potency with anti-CD20 veltuzumab and differentiation from rituximab. Proc Am Soc Clin Oncol, J Clin Oncol. 2008;26:142s(abstract 3043).
13. Leung SO, Goldenberg DM, Dion AS, et al. Construction and characterization of a humanized, internalizing, B-cell (CD22)-specific, leukemia/lymphoma antibody, LL2. Mol Immunol. 1995;32:1413-1427.
14. Goldenberg DM. Epratuzumab in the therapy of oncological and immunological diseases. Expert Rev Anticancer Ther. 2006;6:1341-1353.
15. Mosmann T. Rapid colorimetric assay for cellular growth and survival: application to proliferation and cytotoxicity assays. J Immunol Methods. 1983;65:55-63.
16. Hernandez-Ilizaliturri FJ, Jupudy V, Ostberg J, et al. Neutrophils contribute to the biological antitumor activity of rituximab in a non-Hodgkin's lymphoma severe combined immunodeficiency mouse model. Clin Cancer Res. 2003;9:5866-5873.
17. Melhus KB, Larson RH, Stokke T, Kaalhus O, Selbo PK, Dahle J. Evaluation of the binding of radiolabeled rituximab to CD20-positive lymphoma cells: an in vitro feasibility study concerning low-dose-rate radioimmunotherapy with the alpha-emitter ^{227}Th. Cancer Biother Radiopharm. 2007;22:469-479.
18. Prescribing information for rituximab, 2008. Online document at http://www.rituxan.com/ra/prescribing.info.jsp. Accessed April 24, 2008.
19. Leonard JP, Coleman M, Ketas J, et al. Combination antibody therapy with epratuzumab and rituximab in relapsed or refractory non-Hodgkin's lymphoma. J Clin Oncol. 2005;23:5044-5051.
20. Strauss SJ, Morschhauser F, Rech J, et al. Multicenter phase II trial of immunotherapy with the humanized anti-CD22 antibody, epratuzumab, in combination with rituximab, in refractory or recurrent non-Hodgkin's lymphoma. J Clin Oncol. 2006;24:3880-3886.
21. Leonard JP, Schuster SJ, Emmanouilides C, et al. Durable complete responses with combination therapy of epratuzumab and rituximab: final results of an international multicenter, phase II study, in recurrent indolent non-Hodgkin lymphoma. Cancer. 2008;113:2714-2723.
22. Davis TA, Grillo-Lopez AJ, White CA, et al. Rituximab anti-CD20 monoclonal antibody therapy in non-Hodgkin's lymphoma: safety and efficacy of re-treatment. J Clin Oncol. 2000;18:3135-3143.

23. Nishida M, Usuda S, Okabe M, et al. Characterization of novel murine anti-CD20 monoclonal antibodies and their comparison to 2B8 and c2B8 (rituximab). Int J Oncol. 2007;31:29-40.

24. Polyak MJ, Tailor SH, Deans JP. Identification of a cytoplasmic region of CD20 required for its redistribution to a detergent-insoluble membrane compartment. J Immunol. 1998;161:3242-3248.

25. Polyak MJ, Deans JP. Alanine-170 and proline-172 are critical determinants for extracellular CD20 epitopes: heterogeneity in the fine specificity of CD20 monoclonal antibodies is defined by additional requirements imposed by both amino acid sequence and quaternary structure. Blood. 2002;99:3256-3262.

26. Perosa F, Favoino E, Caragnano MA, Dammacco F. Generation of biologically active linear and cyclic peptides has revealed a unique fine specificity of rituximab and its possible cross-reactivity with acid sphingomyelinase-like phosphodiesterase 3b precursor. Blood. 2006;107:1070-1077.

27. Carnahan J, Stein R, Qu Z, et al. Epratuzumab, a CD22-targeting recombinant humanized antibody with a different mode of action from rituximab. Mol Immunol. 2007;44:1331-1341.

28. Teeling JL, Mackus WJ, Wiegman LJ, et al. The biological activity of human CD20 monoclonal antibodies is linked to unique epitopes on CD20. J Immunol. 2006;177:362-371.

29. Du J, Wang H, Zhong C, et al. Crystal structure of chimeric antibody C2H7 Fab in complex with a CD20 peptide. Mol Immunol. 2008;45:2861-2868.

30. Coiffier B, Lepetre S, Pedersen LM, et al. Safety and efficacy of ofatumumab, a fully human monoclonal anti-CD20 antibody, in patients with relapsed or refractory B-cell chronic lymphocytic leukemia: a phase 1-2 study. Blood. 2008;111:1094-1100.

31. Hagenbeek A, Gadeberg O, Johnson P, et al. First clinical use of ofatumumab, a novel fully human anti-CD20 monoclonal antibody in relapsed or refractory follicular lymphoma: results of a phase I/II trial. Blood. 2008;111:5486-5495.

32. Bleeker WK, Munk ME, Mackus WJM, et al. Estimation of dose requirements for sustained in vivo activity of a therapeutic human anti-CD20 antibody. Br J Haematol. 2007;140:303-312.